PALEOCEANOGRAPHY, VOL. 7, NO. 5, PAGES 529-541, OCTOBER 1992

THE INFLUENCE OF HIGH-LATITUDE SURFACE FORCING ON THE GLOBAL THERMOHALINE CIRCULATION

Thomas F. Stocker

Lamont-Doherty Geological Observatory of Columbia University, Palisades, New York

Daniel G. Wright

Bedford Institute of Oceanography, Department of Fisheries and Oceans, Dartmouth, Nova Scotia, Canada

Wallace S. Broecker

Lamont-Doherty Geological Observatory of Columbia University, Palisades, New York

Abstract. The basin-averaged, latitude-depth ocean model of Wright and Stocker (1992) is used to simulate the deep circulation of the world ocean. Under present-day surface forcing, sinking occurs in the North Atlantic and the southern ocean, and realistic temperature and salinity structures are obtained in the Atlantic, Pacific, and Indian oceans. "Color" tracers and radiocarbon are used to identify the composition of the deepwater masses and the associated renewal time scales. While broad agreement with observations is found in all basins, the water masses in the southern ocean are too young. The global thermohaline circulation and the composition of the deepwater masses are sensitive to the buoyancy contrast between the southern ocean and the North Atlantic. This contrast can be modified by changing relaxation values of temperature and salinity at the northern and southern high latitudes. If the model is forced with the zonal averages of the observed surface salinity, North Atlantic Deep Water is the dominant deep ocean water mass, and hardly any Antarctic Bottom Water flows into the Atlantic. Choosing instead the observed salinities of the newly formed deep water as the restoring values, the model realistically simulates the penetration of Antarctic Bottom Water into the different ocean basins. This has a global effect through reducing both strength and depth of North Atlantic Deep Water formation. If higher surface salinity values are applied in the southern ocean, a steady state is obtained whose tracer distributions and overturning are consistent with reconstructions of the deep circulation during the last glacial maximum. The two states are stable also under mixed boundary conditions and transitions are possible by smoothly varying the surface freshwater flux of one state to that of the other. These experiments suggest the importance of modified high-latitude forcing in glacial-to-interglacial transitions.

Paper number 92PA01695.
0883-8305/92/92PA-01695$10.00

INTRODUCTION

During the last few years a number of modeling studies have confirmed earlier evidence from paleoclimate reconstructions [Broecker et al., 1985; Boyle and Keigwin, 1987; Broecker and Denton, 1989] that the ocean's deep circulation and its variability strongly influence the climate system. In the state that is broadly consistent with present-day observations of temperature, salinity, and various tracer fields, deep water is formed in the northern North Atlantic from where it flows southward and spreads into the different ocean basins. Deep water is also formed around Antarctica and escapes northward into the individual oceans. Return flow is mainly in the thermocline [Gordon, 1986].

The circulation associated with this conveyor belt can be directly measured only in the vicinity of boundary currents. Models are thus important tools for examining the structure of the global ocean circulation. Stommel and Arons [1960] showed analytically that two polar sources of sinking water set up a global deep circulation, and results from three-dimensional [Maier-Reimer and Mikolajewicz, 1989; Marotzke and Willebrand, 1991] and two-dimensional [Stocker and Wright, 1991a, b; Wright and Stocker, 1992] ocean circulation models have simulated this global overturning circulation. It accounts for most of the oceanic poleward heat transport and is an important element of the climate system [Chamberlin, 1906; Weyl, 1968; Broecker and Denton, 1989].

Under mixed boundary conditions, in which sea surface temperatures are relaxed to observed values while surface freshwater fluxes are held constant, a number of distinct circulation modes can be realized. In one of these modes, termed

"Southern Sinking" by Marotzke and Willebrand [1991], deep water is formed only in the southern ocean, and consequently, the thermohaline circulation of the Atlantic is reversed. This state bears some resemblance to a glacial circulation: the region around the North Atlantic receives little or no heat from the ocean, surface waters are cold and very fresh, and the global deepwater masses originate primarily in the southern ocean. However, a disturbing inconsistency with the reconstructions of Boyle and Keigwin [1987] and Duplessy et al. [1988] has remained. Both of these studies emphasize that North Atlantic Deep Water (NADW) formation did not cease during the last glacial maximum but was shallower and weaker than today. Moreover, Duplessy et al. [1988] identify a distinct water mass, "Glacial North Atlantic Intermediate Water," located north of about 15°S and not deeper than 3000 m. Such a water mass is not consistent with the steady "Southern Sinking" state nor with the collapsed state of Manabe and Stouffer [1988]. Useful simulation of climate change using numerical climate models clearly requires that the global overturning circulation and its response to modified forcing be understood and appropriately modeled. It thus remains an important question whether a glacial circulation necessarily implies a different mode of ocean circulation.

The purpose of this paper is threefold. First, an extension of the climate model of Wright and Stocker [1992] (WS92 henceforth) is presented where stable tracers and radiocarbon are included in order to better check the model's performance in the deep ocean. Second, we investigate the sensitivity of the global circulation and the tracer distributions to changes in the surface buoyancy. Here we use the restoring salinities in the southern ocean and the North Atlantic to modify the north-south buoyancy contrast. Within a reasonable range of high-latitude sea surface salinities, the thermohaline circulation can vary smoothly from a state where the deep ocean consists primarily of NADW to one where Antarctic Bottom Water (AABW) dominates the deep ocean. We emphasize that realistic surface forcing in the southern ocean not only determines the properties of AABW but also directly influences the strength and depth of NADW formation. Third, we discuss the paleoclimatic relevance of this result.

Other modeling studies of the global ocean that have included tracers are important benchmarks for the results presented here. Maier-Reimer and Hasselmann [1987] and Bacastow and Maier-Reimer [1990] present inorganic and organic carbon cycle models coupled to their large-scale geostrophic global ocean model using realistic geometry. Largest deviations of the radiocarbon fields from those observed are found in the North Atlantic. Because NADW formation is rather weak in the model (less than 10 Sv versus 15–20 Sv in the modern ocean; $1\,\mathrm{Sv} = 10^6\,\mathrm{m^3 s^{-1}}$), waters in the deep North Atlantic are too old. In more recent versions with modified surface forcing, a NADW formation rate of over 20 Sv and more realistic radiocarbon fields were obtained [Maier-Reimer and Bacastow, 1990].

The Princeton Geophysical Fluid Dynamics Laboratory model has been used in several studies to investigate the composition of the deepwater masses. Cox [1989] used "color" tracers to determine the composition of the deep water as a function of the model's geometry and salinity forcing in the North Atlantic. Only when the salinity forcing in the North Atlantic was enhanced was AABW not the dominant water mass. However, it must be noted that an idealized geometry was considered with an Atlantic basin closed at 60°N. Toggweiler et al. [1989] included radiocarbon in the Princeton model with realistic geometry and found good agreement with the observed data in the Pacific when the model was run in a prognostic mode. However, not enough deep water was formed in the model North Atlantic, and the water was too old especially in the Atlantic below 3000 m and north of 30°S. England [1992] varied the surface salinity in the southern ocean and showed that the formation of Antarctic Intermediate Water (AAIW) as well as the penetration of AABW northward into the basins was more realistic with higher values of surface salinity.

The paper is organized as follows. First, we describe the model and the extensions to include passive tracers. Second, a steady state circulation that is consistent with present-day observations is presented. Finally, we discuss the sensitivity of NADW and AABW formation to high-latitude forcing and its paleoceanographic implications.

MODEL DESCRIPTION

Ocean circulation models in which individual ocean basins are represented by zonally averaged equations are useful tools to simulate the ocean's deep circulation on a global scale. Results are generally consistent with those from three-dimensional general circulation models, in that similar steady states and comparable transient behavior are obtained. The first such model was developed by Marotzke et al. [1988] to reproduce the polar halocline catastrophe found by Bryan [1986]. The latter is a mechanism for fast oceanic reorganizations: small perturbations of the surface freshwater balance cause the polar halocline to extend southward, deep water no longer sinks in high northern latitudes, and the overturning circulation breaks down. These and subsequent models have elucidated the dynamics of the deep circulation and shown that rapid changes can involve the entire volume of the ocean.

The present model is based on Wright and Stocker [1991], where a parameterization of the east-west pressure difference in terms of the meridional pressure gradient was introduced. This parameterization involves a single closure parameter ϵ_0 and accounts for the strong tendency for meridional pressure gradients to be balanced by the Coriolis force. This effect was neglected in the study of Marotzke et al. [1988], and consequently they required a large eddy momentum diffusivity to obtain reasonable overturning transports. As a result, some important features such as surface intensification of the circulation could not be simulated.

The geometry (Figure 1) is similar to that used in the coupled model of Stocker et al. [1992] and the study of WS92. The zonally averaged balances of momentum, mass, potential temperature, and salt are solved in the three major basins of the world ocean. Properties are exchanged through the southern ocean where strong zonal flow results in efficient mixing of intruding water masses. Zonally averaged values thus yield a reasonable representation of the water mass properties in this region. Table 1 gives a summary of the parameter values for the experiments presented here. Throughout this study we use restoring boundary conditions unless otherwise specified; i.e. surface heat (freshwater) fluxes are taken to be proportional to

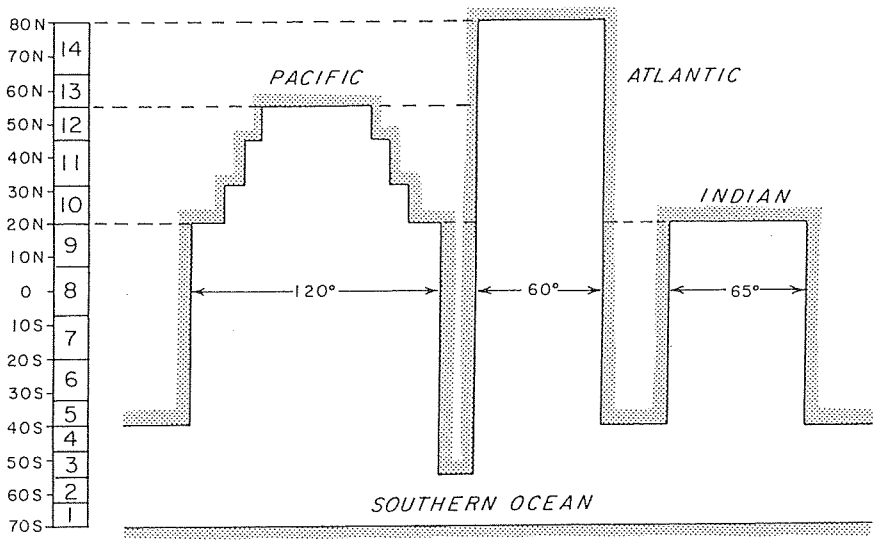

Fig. 1. Geometry of the three zonally averaged ocean basins which join the southern ocean at 40°S. The latitudinal resolution is indicated by the numbered boxes on the left; the vertical resolution is given in Table 1.

TABLE 1. Ocean Model Parameters

	Parameter	Value
f	Coriolis parameter	$2\Omega \sin \phi$
Ω	angular velocity	7.27×10^{-5} s^{-1}
ρ_*	reference density	1027.8 kg m^{-3}
a	Earth's radius	6371 km
g	gravity	9.81 m s^{-2}
K_H	horizontal tracer[a] diffusivity	10^2 m^2 s^{-1}
K_V	vertical tracer[a] diffusivity	10^{-4} m^2 s^{-1}
ϵ_0	closure parameter	0.45
H	ocean depth	5000 m
Δz	mixed layer depth	50 m
	bottom of model cells	50, 100, 150, 250, 500, 750, 1000, 1500, 2000, 2500, 3000, 3500, 4000, 4500, 5000 m
	ridge depth	2500 m
	ridge extent	70°S – 55°S
τ	tracer[a] relaxation time	50 days
λ	decay constant for ^{14}C	3.84×10^{-12} s^{-1}
C^*	restoring surface value for ^{14}C	1000 ppt
τ	relaxation time for ^{14}C	5 years
λ	decay constant for colors	0
AABW	source origin of color	70°S – 62.5°S
AAIW		62.5°S – 40°S
NADW		45°N – 80°N

[a] Tracer denotes potential temperature, salinity, or any of the three color tracers.

deviations of the model surface temperature (salinity) from prescribed values. The model is purely buoyancy driven by relaxing the model temperature and salinity of the uppermost layer to the zonally averaged, annual mean values of Levitus [1982] at 30 m depth. It is known that the observed data are summer biased in locations where a seasonal ice cover is present, and hence the associated forcing density is underestimated. We will show that the present model is sensitive to changes of this forcing and that it can cause global-scale modifications of the thermohaline circulation.

In WS92 a detailed model description was presented which included a nonlinear equation of state, a formulation of wind forcing, and a meridional ridge in the southern ocean. The sensitivities of the T-S characteristics and heat and water fluxes to changes in vertical and horizontal diffusivities as well as the closure parameter ϵ_0 were studied. The focus was mainly on the large-scale circulation and integral quantities such as the meridional heat and water fluxes, characterizing the state of the model climate. Through adjustment of model parameters, without changing the surface water mass properties, a steady state was obtained that compared well with the zonally averaged T-S characteristics of the present-day ocean.

A fully nonlinear, pressure-dependent equation of state is again used here in order to properly model the deep ocean water masses. The static stability is obtained from comparing the in situ densities of two vertically adjacent grid boxes referenced to their intermediate level, and they are mixed when unstable. Horizontal eddy diffusion has been reduced in the present model by decreasing the explicit value and including a scheme that compensates for numerical diffusion. In some of the experiments we have also incorporated a meridional ridge extending from 70°S to 55°S and from 2500 to 5000 m depth, below which a zonal pressure difference can be supported essentially as in the northerly basins. The resulting meridional circulation below the top of the ridge facilitates northward transport of deep water formed around Antarctica. Further model details are discussed in WS92.

The present model version also allows for an arbitrary number of passive tracers. The concentration C of a tracer satisfies the advection-diffusion equation

$$\frac{\partial C}{\partial t} + \frac{1}{a\Lambda\cos\phi}\frac{\partial(\cos\phi\, v\Lambda C)}{\partial\phi} + \frac{\partial wC}{\partial z} = \frac{1}{a^2\Lambda\cos\phi}\frac{\partial}{\partial\phi}(\cos\phi\,\Lambda K_H\frac{\partial C}{\partial\phi}) + \frac{\partial}{\partial z}K_V\frac{\partial C}{\partial z} - \lambda C + q_C^{\text{conv}},$$

where all quantities are zonal averages, (ϕ, z) are latitude-depth coordinates with z positive upwards, Λ is the angular width of the basin, a is the radius of the Earth, (v, w) are the meridional and vertical velocities, and K_H and K_V are the horizontal and vertical diffusivities. The parameter λ is a decay constant and set to $\lambda = \ln 2/5730$ yr for radiocarbon, and $\lambda = 0$ for a stable isotope or a "color" tracer. Vertical fluxes due to convection are denoted by q_C^{conv}.

No-flux conditions for a tracer are applied at the bottom and the lateral boundaries of the basin, while at the surface we assume restoring boundary conditions; i.e.,

$$F = \frac{\Delta z}{\tau}(C - C^*)\,,$$

where F is the vertical tracer flux (positive upward), Δz is the depth of the mixed layer, and C^* is a tracer concentration to which the model's surface value is relaxed on the time scale τ. All tracers (including temperature and salinity) except radiocarbon are relaxed to specified values over a time scale of 50 days. For radiocarbon this relaxation time is 5 years for the present mixed layer depth [Toggweiler et al., 1989].

While radiocarbon allows us to compare the overturning time scales of the deep circulation, stable "color" tracers are useful in determining the composition of the deep water according to their production site. Where a particular color is released at the ocean surface the relaxation concentration C^* is set to 100 and $C^* = 0$ everywhere else. Provided each surface box of the ocean is assigned one and only one stable color, the sum over all color concentrations at any location in the ocean tends to 100 after a few thousand years (i.e., a few times the global overturning time scale). The mixture of water masses can then be conveniently analyzed. The same diagnostic instrument has been used previously by Cox [1989] and E. Maier-Reimer (personal communication, 1991), and we chose latitude bands for the different colors similar to Cox [1989]. In the following, four colors are used: AABW is formed south of 62.5°S, AAIW between 62.5°S and 40°S, NADW is originating north of 45°N, and "other" waters form over the remaining surface area. Note that the fourth tracer need not be explicitly carried in the model calculations as long as we are not concerned with the initial spin-up period before all water parcels have passed through the surface layer.

STEADY STATES

The three-basin model is spun up from rest by restoring surface temperature and salinity to the zonal averages of Levitus [1982]. The values of salinity suggested by Levitus [1982] for the southernmost box of the southern ocean and the northernmost box of the North Atlantic are 34.0 and 34.6 ppt, respectively. In these two regions, the model forms deep water, and thus it is important for the deep ocean characteristics that the sinking water masses have approximately the right salinity. Using these surface values for the forcing, however, yields a state in which NADW is the dominant water mass in the entire Atlantic basin and too strong in the Pacific and Indian oceans. Color tracers and radiocarbon show clearly that the composition of the deepwater masses is not satisfactory, and the southern ocean is too fresh. Two factors contribute to this discrepancy. First, deepwater formation associated with salinity enhancement due to the production of sea ice is not included in our model. This large-scale effect is particularly important in the southern ocean. Second, the east-west variation in surface water mass properties, and hence in deepwater mass production, in the North Atlantic is not represented by our zonally averaged model. Fortunately, the north-south variation in water mass properties is much greater than the east-west variation with the result that this latter effect does not dominate the solutions. To remove the above discrepancy, we simply modify the forcing salinities in the southern ocean and North Atlantic to 34.6 and 35.0 ppt, respectively. These are typical observed salinities at about 1000 m depth in these regions. England [1992] has used a similar modification in a global general circulation model to improve AABW and AAIW formation.

A diagnosis of this steady state after 10,000 years (20,000 for ^{14}C) of integration is carried out giving the latitude-depth fields of the overturning mass transport stream function, potential temperature, salinity, the stable color tracers, and radiocarbon (Figure 2) . The maximum overturning in the North Atlantic attains 24 Sv, half of which flows into the southern ocean between 2000 and 3000 m depth. About 40 Sv AABW are created, of which 5 Sv flow into the Atlantic spreading to 45°N. Deep convection from top to bottom occurs in the northernmost and southernmost cells of the model. Pacific and Indian oceans both show broad upwelling closing the conveyor belt circulation.

Potential temperature and salinity are in good quantitative agreement with the zonal averages of Levitus [1982] showing a deep North Atlantic warmer than the Pacific and Indian oceans (Figure 2). The influences of the Mediterranean and Red seas are not included, but WS92 show that their effect on global conditions is minimal, at least under the present restoring boundary conditions. The salinity field of the Atlantic is distinctly different from that in the other basins, consistent with the data. Both AAIW and AABW as well as NADW are apparent in this basin. The latter water mass shows up as a local salinity maximum at 40°S and 3000 m depth in the Pacific and Indian oceans. This feature is clearly visible in the observed fields of the Indian Ocean; however, the lack of zonal resolution in the model's southern ocean results in a larger influence of NADW in the Pacific Ocean than observed.

As discussed above, three distinct high-latitude water masses are identified by color tracers: AABW, AAIW, and NADW (Figure 2). While AABW is the dominant water mass in the Pacific and the Indian oceans where it rises close to the surface, its northward spreading in the Atlantic is hindered by NADW which has a slightly higher density north of 45°N. Spreading of AAIW is also different in the three basins. In the Pacific Ocean it is restricted to the southern hemisphere, while in the Indian Ocean and particularly the Atlantic it penetrates further to the north. In the Atlantic basin, AAIW is mixed with the recirculating NADW which helps carry the influence northward at shallower depths. WS92 suggest, however, that inclusion of the Mediterranean would modify the latter result. The penetration of NADW into the other basins is evident in the color tracer contours and occurs at about 3000 m depth. Qualitative agreement with Cox [1989] is found. However, the presence of NADW in the deep ocean is much stronger and probably more realistic in the present model than in the Cox model.

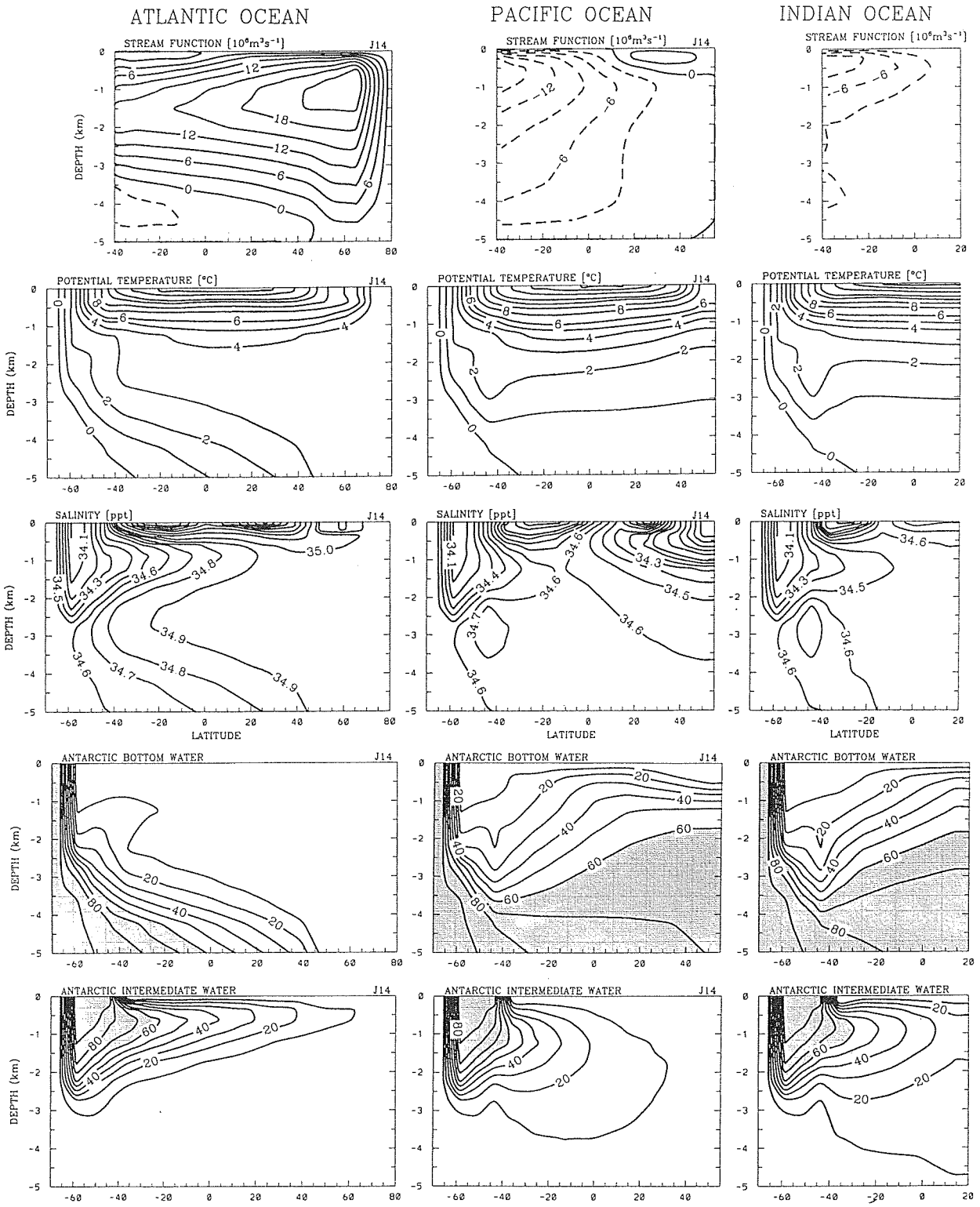

Fig. 2. Latitude-depth sections of the overturning stream function (in Sverdrup, $1\,\mathrm{Sv} = 10^6\ \mathrm{m^3\,s^{-1}}$), potential temperature, salinity, percent concentration of Antarctic Bottom Water (AABW), Antarctic Intermediate Water (AAIW), and North Atlantic Deep Water (NADW); concentrations exceeding 60% are shaded. Radiocarbon is given in parts per thousand depletion from a standard value.

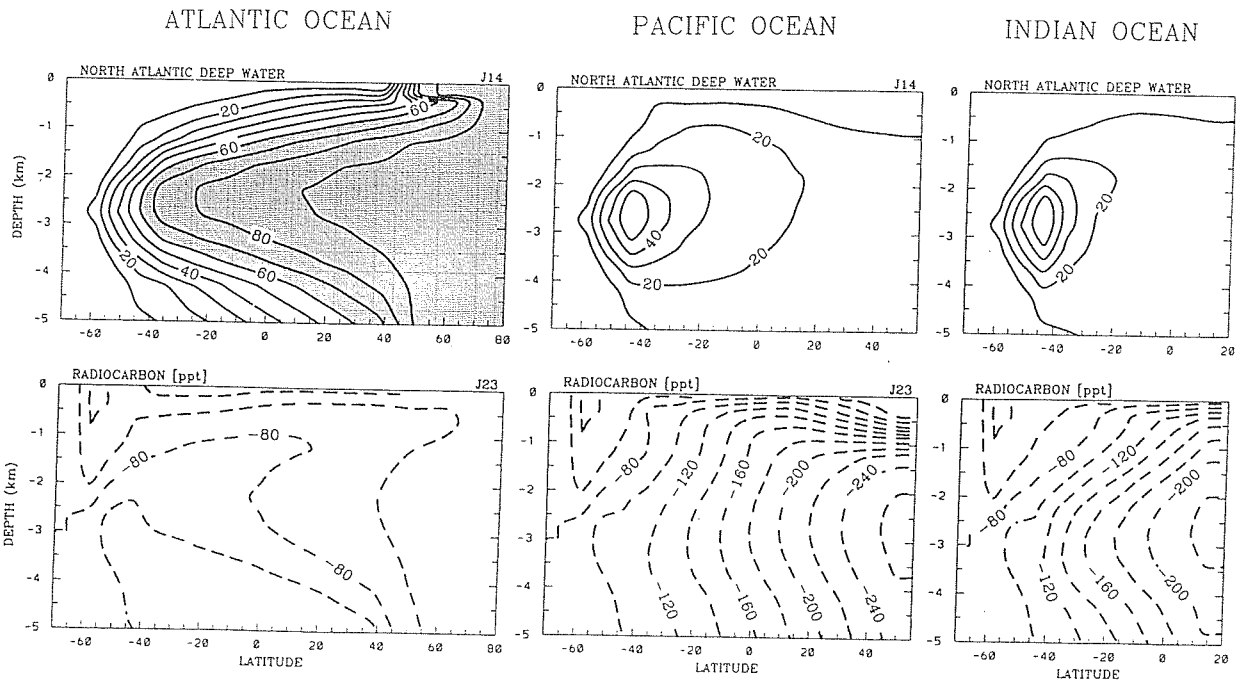

Fig. 2. (continued)

Consistent with this, Toggweiler et al. [1989] show large deviations of the radiocarbon fields from those observed in the North Atlantic. This is caused by weak NADW formation that penetrates only down to about 2500 m depth. The concentration of those water masses that are formed between 40°S and 45°N (55°N in the Pacific) does not exceed 20% below 1500 m in the Pacific, 1000 m in the Indian Ocean and 700 m in the Atlantic Ocean (not shown in Figure 2).

The radiocarbon contours can be compared to the data given in the work by GEOSECS [1987] at depths that are not affected by bomb-produced radiocarbon (Figure 2). The agreement is reasonably good in that the model reproduces the qualitatively different structures in the three ocean basins. The most significant discrepancy is that the waters tend to be too young in the southern ocean. This indicates that the surface residence time of the source waters for this region may be too long. We have done an additional set of experiments where the meridional resolution of the model between 55°S and 70°S has been doubled and three marginal seas south of 70°S have been added. The global thermohaline circulation is not sensitive to these refinements, but increased meridional resolution allows some of the deep water formed in the southern locations to upwell and recirculate south of 60°S. This provides a mechanism to reduce the residence time at the surface, but it is not sufficient to produce significantly older waters in the deep southern ocean.

In addition to the young ages observed in the southern ocean, the ages tend to be somewhat too old in the Pacific. However, the data to which comparison can be made is not zonally averaged. It is thus not surprising that the model does not show the strong vertical gradients of $\Delta^{14}C$ as found in the western section (about 175°W) of the data. This is the signature of the deep western boundary current entering the Pacific. Consistent with this argument are weaker vertical gradients found in the eastern section (roughly 130°W) and the general NW-SE orientation of lines of constant $\Delta^{14}C$ at 4000 m depth [e.g., Fiadeiro, 1982]. The zonally averaged model does not reproduce such zonal structure.

The state given in Figure 2 is very similar to the steady state of the base climate given in WS92 in terms of the climatically relevant fluxes (meridional oceanic heat and freshwater fluxes). However, the composition of the deepwater masses is distinctly different here. By increasing the surface restoring salinity in the southern ocean, the influence of NADW is considerably reduced and brings the tracer fields generally closer to the observed distributions. It would be possible to introduce spatial variability of now constant parameters (e.g., the proportionality constant relating the east-west pressure difference to the meridional pressure gradient, vertical and horizontal diffusivities) to further improve the fields. However, we have abstained from introducing such subjective tunings and prefer to put up with the remaining few quantitative differences. Some differences are necessarily involved with a zonally averaged model.

Comparison of T-S properties of AABW, AAIW, and NADW where their concentrations exceed 60% in the associated color shows that the three water masses are distinct with the biggest scatter in AAIW reflecting mixing with the upper water masses of the different ocean basins (Figure 3) . AABW is the best defined water mass indicating only weak mixing. NADW is confined within two mixing lines that intersect at the (S,T) of the deep convecting region in the North Atlantic. The steep mixing line represents the incoming thermocline water, whereas the almost isopycnal mixing line is influenced by AABW.

The state described above is consistent with present-day oceanic conditions. However, ocean models can have multiple equilibria when forced with mixed boundary conditions;

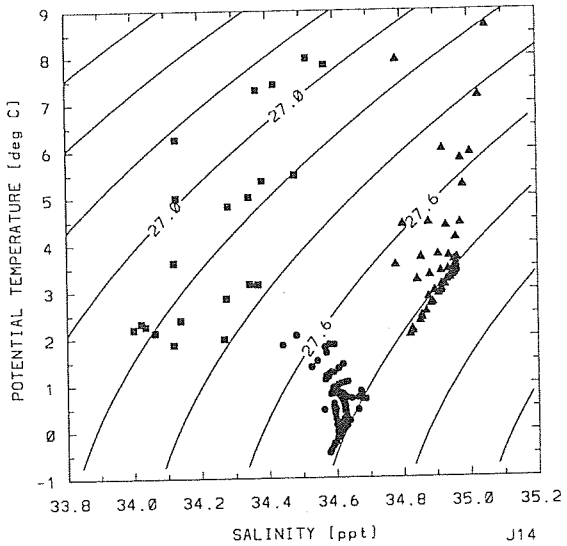

Fig. 3. T-S distribution of the three main water masses in the model for the state given in Figure 2. NADW is denoted by triangles, AABW by circles, and AAIW by squares.

i.e. sea surface temperature is still relaxed to prescribed values, while surface freshwater fluxes are held constant. One of the possible states, referred to as the "Southern Sinking" state [Marotzke and Willebrand, 1991; Stocker and Wright, 1991a, b], has a reversed Atlantic circulation and a strong polar halocline in the North Atlantic which extends southward to about 25°N. The Atlantic tracer fields become "Pacific-like" with the lowest $\Delta^{14}C$ found in its deep northern part. Figure 4 gives

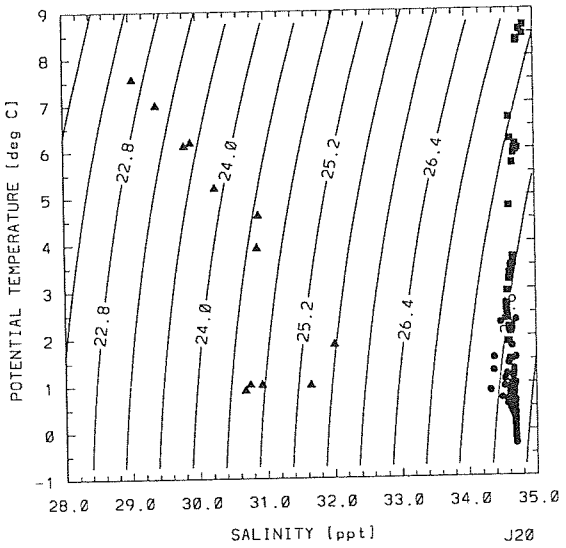

Fig. 4. As Figure 3 but for the "Southern Sinking" state that represents the second equilibrium under the mixed surface boundary conditions. AABW (circles) and AAIW (squares) have about the same salinity, while the waters originating from the North Atlantic (triangles) are extremely fresh. This indicates a major rearrangement of salt in the global ocean.

the T-S properties of this state: NADW has disappeared, and surface waters north of 45°N in the Atlantic are very fresh; AAIW is now as salty, but warmer than AABW demonstrating global-scale redistributions of salinity.

It was hypothesized in earlier studies [e.g., Maier-Reimer and Mikolajewicz, 1989; Stocker and Wright, 1991a] that the Southern Sinking state might be a candidate for the deep ocean circulation during the last glacial maximum or during the Younger Dryas climate event. This was to some extent supported by several characteristics reconstructed from sediment cores and other paleoclimatic evidence around the North Atlantic basin. The most important facts, the rapid transitions between different climates, the abrupt terminations, and the sudden shutdown of the oceanic meridional heat flux, could be explained by flips between multiple equilibria. However, the inconsistency with the conclusions of both Bolye and Keigwin [1987] and Duplessy et al. [1988], that NADW formation has never completely vanished and that a distinct intermediate water mass in the North Atlantic existed, has always remained. Below we show that a circulation consistent with the paleoceanographic observations can be realized through rather modest modifications of the buoyancy contrast which is present between the southern ocean and the North Atlantic in the global conveyor belt circulation (Figures 2 and 3).

SURFACE FORCING IN THE SOUTHERN OCEAN AND NORTH ATLANTIC

Obtaining a realistic composition of the deepwater masses in the world ocean is essential if one is interested in integrations over time scales longer than the exchange time of the oldest waters ($\approx$ 1800 years) [Stommel and Arons, 1960] or when transient, glacial-to-interglacial experiments are performed. Many three-dimensional general circulation models forced with the observed climatology show rather weak and shallow formation of NADW and systematic deviations of the deep water properties. Unfortunately, it is in the regions where deep waters are formed that surface observations are least reliable and physical processes are most complicated. Some uncertainty therefore exists as to what values of the surface salinity and temperature should be used to simulate present oceanic conditions using restoring boundary conditions, which themselves are only crude parameterizations of exchange processes at the surface. This is particularly true when seasonal variations are not resolved and the uncertainty is, of course, increased for paleoceanographic simulations.

Using a simpler but dynamical model for the thermohaline circulation we investigate the sensitivity of the global circulation to variations in the surface buoyancy forcing at high latitudes under restoring boundary conditions. These changes can also be simulated under mixed boundary conditions by small global changes in the surface water balance (see below).

Here we concentrate on the influence of salinity variations, but it should be noted that changes in surface heat flux may have similar effects. Let S_1^* and S_2^* denote the restoring surface salinities south of 62.5°S and north of 65°N (boxes 1 and 14 in Figure 1), respectively. Figure 5 gives the maximum inflow of AABW at 40°S as a function of the restoring surface salinity S_1^* for 5 sets of steady states. The characteristics of sets A to E are given in Table 2 . Inclusion of a meridional ridge in the southern ocean is important in increasing the magnitude as

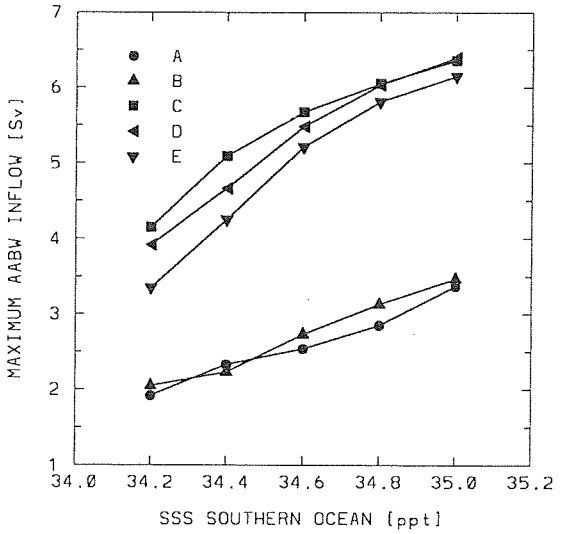

Fig. 5. Maximum inflow of AABW (in Sverdrup) at 40°S into the Atlantic as a function of the restoring surface salinity south of 62.5°S. Inflow is generally increased in magnitude when the buoyancy forcing in the southern ocean is stronger but reduced if there is no meridional ridge in the southern ocean. The restoring salinity north of 65°N has little influence (sets A and B). Increasing horizontal diffusivity decreases the magnitude of this exchange (sets C – E).

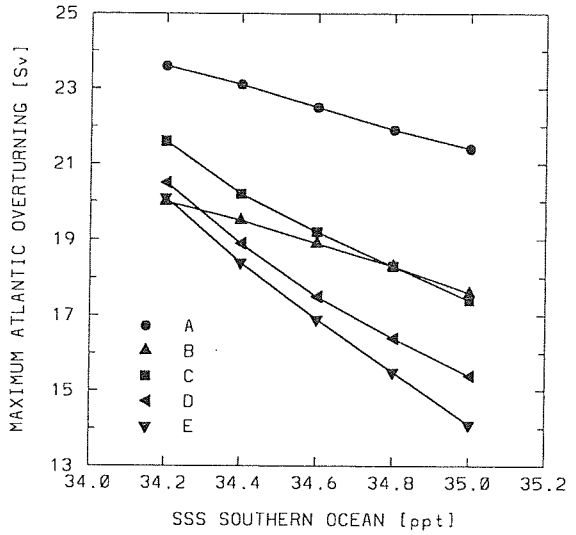

Fig. 6. Overturning in the North Atlantic (in Sverdrup) as a function of the restoring surface salinity south of 62.5°S. Stronger buoyancy forcing in the southern ocean decreases NADW formation, and a ridge increases this sensitivity. The strongest sensitivity is due to the buoyancy forcing north of 65°N (sets A and B).

well as the sensitivity of AABW inflow. Neither modification of S_2^* (sets A and B) nor increasing horizontal diffusivity (sets C to E) have such a large influence on AABW inflow.

NADW formation rates show significantly different dependencies (Figure 6) . As expected, reduction of S_2^* considerably decreases NADW formation. By facilitating intrusion of AABW into the Atlantic which modifies the density structure in the deep ocean, the topographic ridge reduces overturning and also increases the sensitivity to S_1^*.

The mechanism by which high-latitude forcing influences the global overturning is related to the modification of the meridional density gradient when the properties of the forming deep water are changed. The density difference $\Delta\sigma$ between the deep convecting water in the northern North Atlantic and in the southern ocean provides a rough measure of the related circulation in the Atlantic basin if the forcing at all other locations is unchanged. This difference is positive for the unmodified Levitus values, and NADW dominates the whole deep ocean. When S^* is increased in both locations to the values of the observed underlying deepwater masses, $\Delta\sigma$ decreases due to the larger salinity increase in the southern ocean, and for $S_1^*=S_2^*$ it becomes negative due to lower temperatures. The Atlantic overturning stream function for $\Delta\sigma > 0$ (Figure 2) and for $\Delta\sigma < 0$ (Figure 7) are quantitatively different from each other particularly at depths below 3000 m .

TABLE 2. Parameter Values and Topography for the Five Sets of Experiments Considered in Figures 5 and 6

	Topography	S_2^*, ppt	K_H, $m^2 s^{-1}$
A	no ridge	35.0	100
B	no ridge	34.6	100
C	ridge	35.0	100
D	ridge	35.0	500
E	ridge	35.0	1000

The diagnosis for a case where $S_1^*=S_2^*=35$ ppt is considered next (Figure 7). In the Pacific and Indian oceans only the strength of NADW inflow is diminished, but the other fields have not changed much compared to Figure 2. The Atlantic circulation, however, is weaker and much shallower due to the increased density of AABW. This water mass occupies the entire deep ocean below 3000 m depth and penetrates far north in the Atlantic. Old water (large negative values of $\Delta^{14}C$) is now located where the youngest waters used to be, and a strong vertical gradient of radiocarbon or age is present in the northern latitudes of the Atlantic.

Such a gradient could also be observed in other tracers (e.g., phosphorus or $\delta^{13}C$) which distinguish waters formed in the southern ocean from those formed in the North Atlantic. Boyle and Keigwin [1987] estimated a glacial Atlantic phosphorus profile at 41°N using cadmium/calcium ratios and found a pronounced vertical gradient that is absent in today's observations. This is supported by Duplessy et al. [1988] who reconstructed Atlantic $\delta^{13}C$ during the last glacial maximum. The tracer distributions given in Figure 7 are consistent with these observations and suggest that the deep circulation of the glacial ocean may have been in a similar circulation mode. Deep ocean salinity is about 0.2 ppt higher in the "glacial" mode (Figure 7) than in the model's present-day mode (Figure 2) resulting in higher global salinity for the glacial state. The total salinity difference between the two modes is equivalent to about 7×10^6 km^3 of melted ice which is only about 10% of the total estimated ice

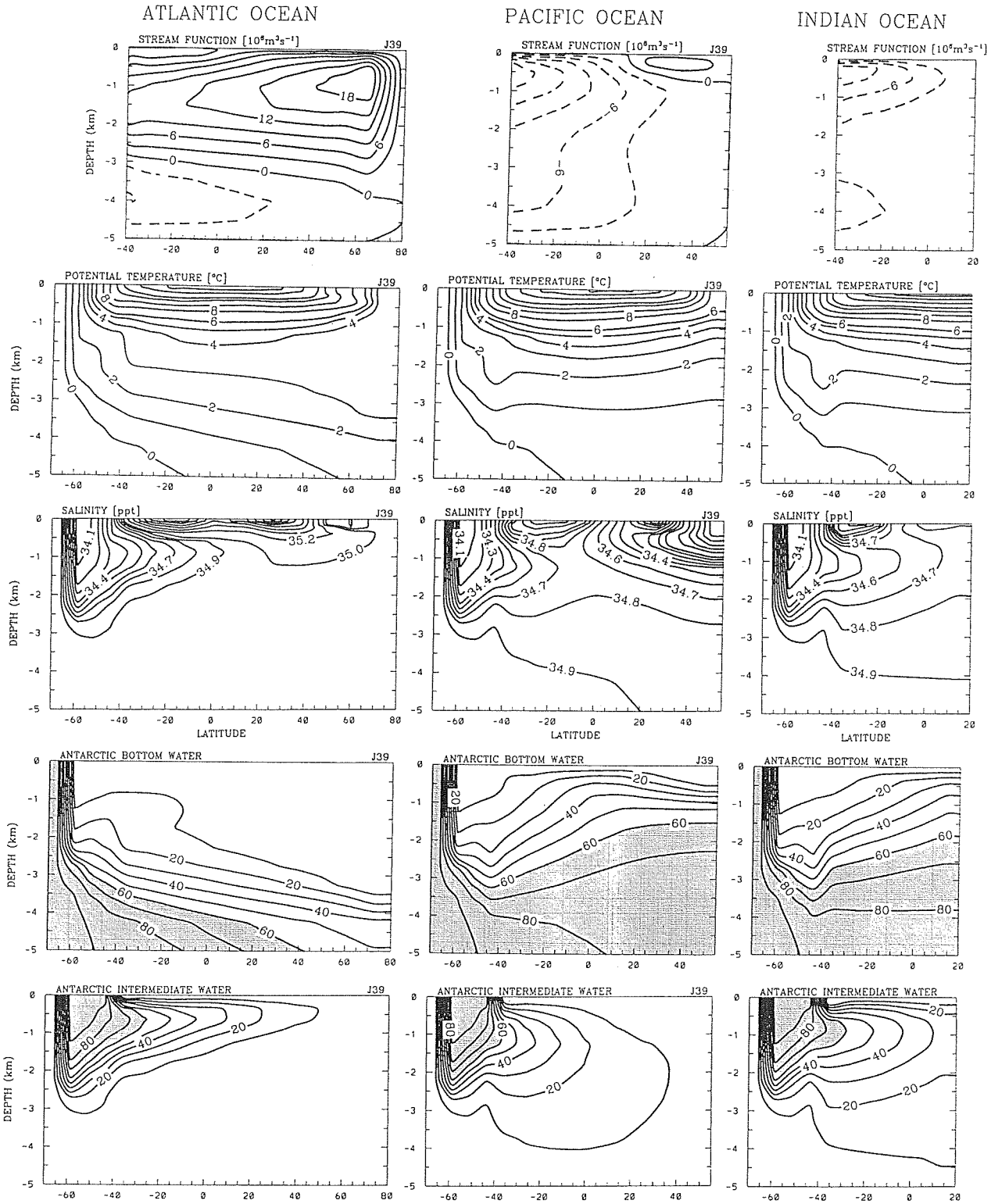

Fig. 7. As Figure 2 for the "glacial mode" of the thermohaline circulation in the world ocean. The deep ocean is cooler and more saline than the modern state because AABW is more dominant. The influence of NADW in the Pacific and Indian oceans is reduced. The deep North Atlantic is occupied by older water originating from the southern ocean, and stronger vertical property gradients are present.

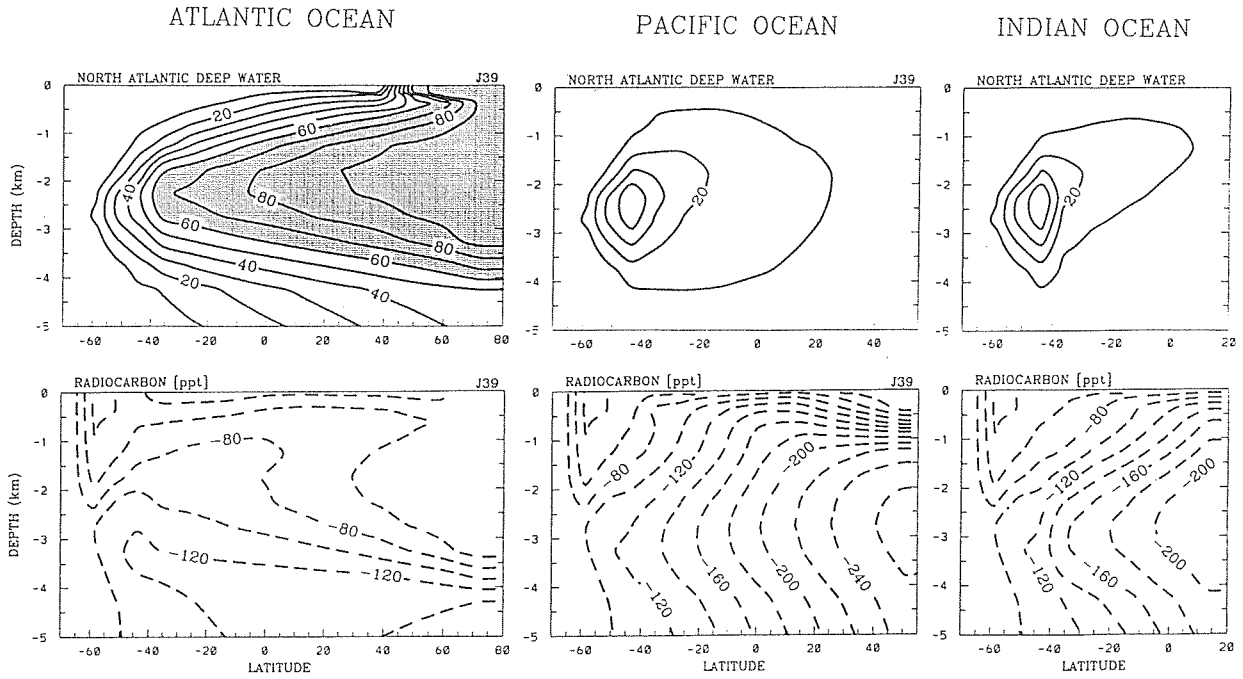

Fig. 7. (continued)

tropical Atlantic must have been older by about 320 ± 80 years. This is consistent with the age difference estimated from the two states presented in Figures 2 and 7 (Figure 8) . The deep Atlantic waters are progressively older northward in the glacial state. Compared to Broecker et al. [1990] the age difference in the tropical Atlantic is probably too low in the model. In the tropical deep Pacific, on the other hand, the age difference is only about 50 years. The general agreement between model and observations supports the suggestion that the glacial overturning circulation was similar to Figure 7.

The computational efficiency of the present model allows us to perform a sensitivity study over a wide range of the buoyancy forcing of both the southern ocean and the northern North Atlantic. The restoring salinities S_1^* and S_2^* have been independently varied in the range of $33.5\,\text{ppt} \leq S_1^*, S_2^* \leq 35.5\,\text{ppt}$. The steady state transport stream function maximum associated with AABW inflow into the Atlantic basin is illustrated in Figure 9 and the maximum value of the overturning stream function in the Atlantic basin is given in Figure 10 . Consistent with the results in the previous section, larger S_1^* (S_2^*) increases (decreases) the AABW influx in magnitude, with greater sensitivity to S_1^* than to S_2^*. Similarly, larger S_2^* (S_1^*) increases (decreases) the maximum overturning rate in the Atlantic with greater sensitivity to S_2^*.

For sufficiently low values of either S_1^* or S_2^*, convection in the corresponding cell is abruptly reduced and the deep density field is then influenced only little by further reductions. The effect is evident in Figures 9 and 10 for North Atlantic salinities less than about 33.9 ppt. For southern ocean salinities the cutoff value increases from about 33.7 ppt at the lowest values of North Atlantic salinity to 34.0 ppt at the highest values plotted. It should be noted that when S_1^* and S_2^* take volume during the peak of the last glacial [Denton and Hughes, 1981].

Further evidence about the state of the glacial ocean comes from the study of Broecker et al. [1990], who established the differences in distribution of radiocarbon between the glacial and the modern ocean. They found that, within the uncertainty of the measurements, the waters of the deep tropical Pacific had about the same age as today, while the waters of the deep such low values, the densest water masses will be produced in the neighboring surface boxes. Thus, if the reduction of surface salinity were extended equatorward, the sensitivity would reach to lower salinity values until convection is reduced in all columns affected.

It is clear (Figures 9 and 10) that the deep ocean circulation reacts to changes of the buoyancy forcing at the locations where the deep waters of the global ocean are produced. This emphasizes the importance of the buoyancy contrast between these regions. Changes are such that one extreme state has NADW dominating the deep water, while in the other AABW is the prominent deepwater mass. We have done an additional experiment with S_1^*=34.7 ppt and S_2^*=28.0 ppt as observed in the "Southern Sinking" state. Note that the "Southern Sinking" was obtained under mixed boundary conditions, while here we use the restoring type, and only the highest-latitude surface salinities are modified. Under this extreme forcing, a state similar to the Southern Sinking results where Atlantic overturning is very weak and confined to the upper 1000 m. Obviously, the restoring conditions at the other latitudes prevent major meridional shifts of salt in the Atlantic as is possible for the mixed type, and hence a full reversal of the deep circulation is not obtained. Nevertheless, this illustrates that the "Southern Sinking" is an extreme state where the buoyancy forcing in the

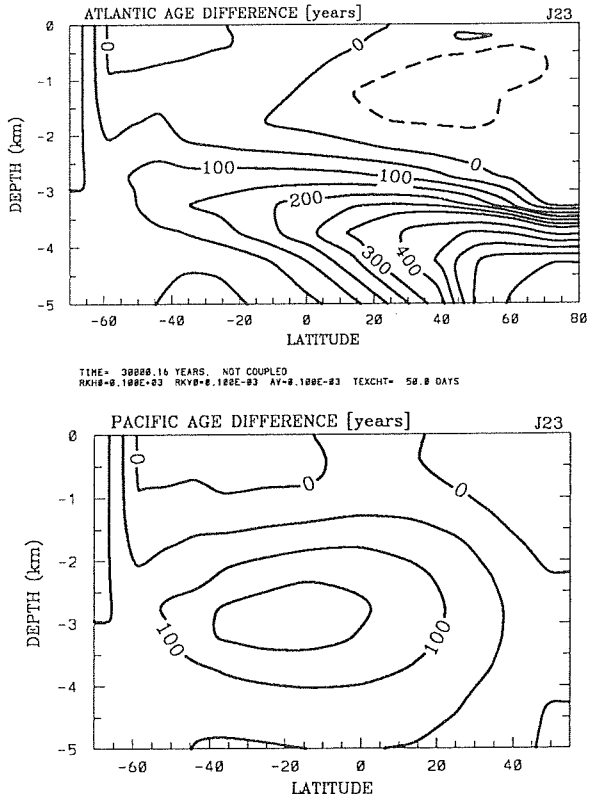

Fig. 8. Age difference (in years) of the water masses between the glacial state of Figure 7 and the modern state of Figure 2. The age difference is given by $\lambda^{-1}\ln[(1000 + \Delta^{14}C|_{modern})/(1000 + \Delta^{14}C|_{glacial})]$, and positive values indicate that waters in the glacial ocean are older than those in the modern ocean. Contour interval is 50 years for ages less than 300 years and 100 years otherwise.

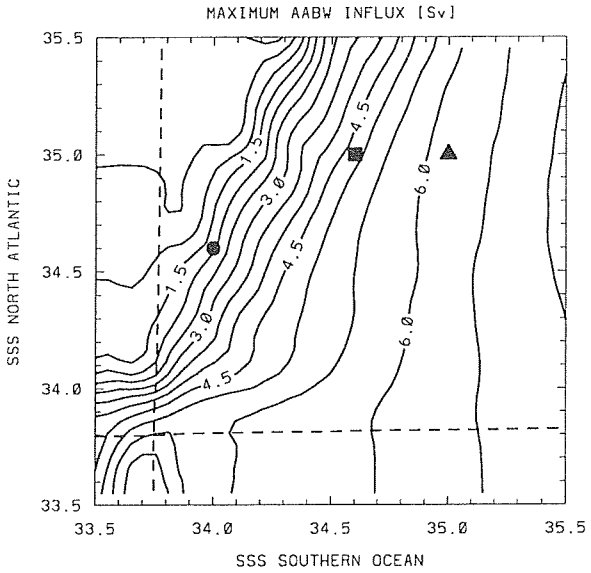

Fig. 9. Contours of the mass transport stream function associated with inflow of AABW (in Sverdrup) at 40°S into the Atlantic as a function of the restoring surface salinity south of 62.5°S and north of 65°N. Except for the case of a very fresh southern ocean the inflow is most sensitive to southern ocean buoyancy forcing. Symbols denote steady states forced with the zonal averages of Levitus (dot), a state consistent with the modern (square) and with the glacial deep circulation (triangle). Dashed lines indicate equality of the forcing density of boxes 1 and 2, and 13 and 14, respectively.

southern ocean is dominant. The "glacial" state (Figure 7) has a north-south buoyancy contrast that lies between that of the conveyor belt and that of the Southern Sinking mode.

The above results are obtained using restoring surface boundary conditions. Previous models of the global thermohaline circulation have employed mixed boundary conditions in order to better represent atmosphere-ocean interactions. The presence of multiple equilibria and, to some extent, the strong sensitivity of these models to changes of the surface freshwater balance, are a consequence of these mixed boundary conditions. It is thus important to investigate whether transitions between the "glacial" and the "modern" state are possible in this model when mixed boundary conditions are used.

We have performed two experiments beginning from the steady states of Figures 2 and 7, respectively. After 1000 years of intergration under mixed boundary conditions, a transient period of 1000 years was started during which the surface freshwater fluxes were gradually changed to those diagnosed from the other state. In this model a change from a glacial (Figure 7) to a modern circulation (Figure 2) involves an increase of the hydrological cycle: the modern meridional transport of freshwater into the southern ocean is stronger by about 0.16 Sv, to which Pacific (0.08 Sv), Atlantic (0.04 Sv), and Indian (0.04 Sv) oceans contribute. The resulting circulation was then integrated for another 5000 years. Both experiments showed the expected transition from one state to the other without involving abrupt changes or reversals of the Atlantic circulation. This demonstrates that despite the presence of multiple equilibria under mixed boundary conditions, relatively smooth transitions between "glacial" and "modern" (and vice versa) states can be realized.

CONCLUSIONS

The deep ocean circulation model of WS92 was extended to include stable and unstable tracers. Under present-day forcing, a conveyor belt circulation results which yields overturning, temperature, salinity and radiocarbon fields that are broadly consistent with the data of the modern ocean. The Atlantic Ocean contains NADW over much of the water column, with a mixture of recirculating NADW and AAIW above 2500 m and AABW intruding at depth into the northern hemisphere. In the Pacific and Indian oceans, AABW and AAIW are the dominant water masses, while NADW mixes in across 40°S at about 3000 m depth.

We have followed Cox [1989] and employed three high-latitude color tracers to determine the mixture of water masses formed at different locations. If the model is forced with the Levitus [1982] annual mean values of salinity in the high latitudes (where a seasonal ice cover may be present), the model

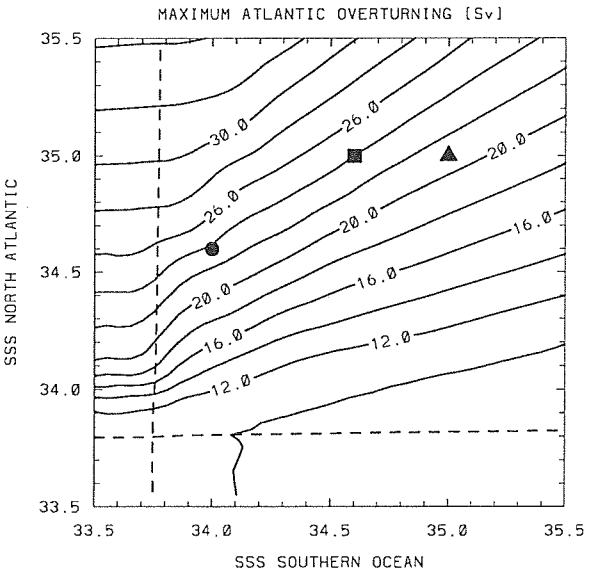

Fig. 10. Contours of overturning in the North Atlantic (in Sverdrup) as a function of the restoring surface salinity south of 62.5°S and north of 65°N. Stronger buoyancy forcing in the North Atlantic (southern ocean) increases (reduces) NADW formation. Symbols denote steady states forced with the zonal averages of Levitus (dot), a state consistent with the modern (square) and with the glacial deep circulation (triangle). Dashed lines indicate equality of the forcing density of boxes 1 and 2, and 13 and 14, respectively.

overestimates the influence of NADW, and little AABW penetrates northward into the ocean basins. Consequently, contours of radiocarbon bear little resemblance with those observed. However, the surface data at high latitudes are based on only a few observations and are most likely summer biased, resulting in inaccurate buoyancy forcing at these latitudes. Increased restoring salinities in both high latitudes (south of 62.5°S and north of 65°N) to values typical of the newly formed deep water produce more realistic property fields throughout the ocean.

This suggested a sensitivity study testing the influence of surface density in the deepwater formation areas on the global thermohaline circulation. By increasing restoring salinity, deepwater formation increases locally and fills the deep ocean with more saline water. This also modifies the meridional density gradient which drives the deep circulation. It is through this mechanism that the salinity of the newly produced deep water can have important effects on global climate.

Increasing the salinity in the formation region for AABW can cause it to flow much further northward into the Atlantic and makes NADW formation both weaker and shallower. Modifying this salinity by about 0.4 ppt suffices to produce a global deep circulation that is in many aspects consistent with the situation during the last glacial maximum. Boyle and Keigwin [1987], Duplessy et al. [1988], and Broecker et al. [1990] have found that the glacial ocean is characterized by a reduced and much shallower NADW production, with deep water originating mainly from the southern ocean. This leads to vertical tracer gradients that are significantly increased during the glacial compared to the modern Atlantic Ocean. The state that is obtained in the present model when the buoyancy forcing in the southern ocean is increased, reproduces these findings.

What has been varied here was a parameter external to the model formulation. However, the essential quantities modified are the densities of the newly formed deep waters in the southern ocean and the North Atlantic. While we have chosen to focus on salinity variations, similar effects would be associated with temperature variations and in reality, both probably play significant roles. In the climate system, salinity enhancement at high latitudes is the result of ice formation and brine rejection caused by seasonal variations in ice cover. Sea ice also acts as an insulator, reducing the air-sea heat exchange. Incorporation of a sea ice model is part of ongoing research. The present results highlight the global importance of high-latitude buoyancy forcing, and show the profound impact that such modifications can have. Within reasonable ranges of this forcing, circulations can be obtained that show substantially different tracer distributions in the deep ocean. For present-day values of the surface forcing a modern circulation results, while increasing AABW density relative to NADW density results in a state which is in many aspects consistent with oceanic conditions during the last glacial maximum.

Finally, we have demonstrated that it is possible to simulate transitions between the two states also under mixed boundary conditions. This can be achieved by smoothly changing the surface freshwater fluxes diagnosed from one state to those diagnosed from the other state. During this transient period, the thermohaline circulation exhibits a smooth evolution. Abrupt changes of the global thermohaline circulation, on the other hand, occur as a result of transitions between multiple equilibria as demonstrated in many earlier studies. However, large-scale and long-term changes in the hydrological cycle (through changes of sea ice or evaporation/precipitation) can also contribute to global changes of the thermohaline circulation.

Acknowledgements. We have benefitted from discussions with R. G. Fairbanks and D. G. Martinson and from comments by two anonymous reviewers. Fritz Zaucker helped with the LaTeX style file provided by John Wilkin; Patty Catanzaro improved the figures. This study was made possible by grant DE-FG02-91ER61202 of the U.S. Department of Energy. This is Lamont-Doherty contribution # 4958.

REFERENCES

Bacastow, R., and E. Maier-Reimer, Ocean-circulation model of the carbon cycle, *Climate Dyn.*, *4*, 95-125, 1990.

Boyle, E. A., and L. Keigwin, North Atlantic thermohaline circulation during the past 20,000 years linked to high-latitude surface temperature, *Nature*, *330*, 35-40, 1987.

Broecker, W. S., and G. H. Denton, The role of ocean-atmosphere reorganisations in glacial cycles, *Geochim. Cosmochim. Acta*, *53*, 2465-2501, 1989.

Broecker, W. S., D. M. Peteet, and D. Rind, Does the ocean-atmosphere system have more than one stable mode of operation?, *Nature*, *315*, 21-26, 1985.

Broecker, W. S., T-H. Peng, S. Trumbore, G. Bonani, and W. Wölfli, The distribution of radiocarbon in the glacial ocean, *Global Biogeochem. Cycles*, *4*, 103-117, 1990.

Bryan, F., High-latitude salinity effects and interhemispheric thermohaline circulations, *Nature, 323*, 301-304, 1986.

Chamberlin, T. C., On a possible reversal of deep-sea circulation and its influence on geologic climates, *J. Geol., XIV*, 363-373, 1906.

Cox, M. D., An idealized model of the world ocean, Part I, The global-scale water masses, *J. Phys. Oceanogr., 19*, 1730-1752, 1989.

Denton, G. H., and T. J. Hughes, *The Last Great Ice Sheets*, 484 pp., John Wiley, New York, 1981.

Duplessy, J. C., N. J. Shackleton, R. G. Fairbanks, L. Labeyrie, D. Oppo, and N. Kallel, Deepwater source variations during the last climatic cycle and their impact on the global deepwater circulation, *Paleoceanography, 3*, 343-360, 1988.

England, M., On the formation of Antarctic intermediate and bottom water in ocean general circulation models, *J. Phys. Oceanogr., 22*, 918-926, 1992.

Fiadeiro, M. E., Three-dimensional modeling of tracers in the deep Pacific Ocean. II. Radiocarbon and the circulation, *J. Mar. Res., 40*, 537-550, 1982.

GEOSECS, *Atlantic, Pacific and Indian Ocean Expeditions*, Vol. 7, *Shorebased Data and Graphics*, 200 pp., National Science Foundation, Washington, D. C., 1987.

Gordon, A.L., Interocean exchange of thermocline water, *J. Geophys. Res., 91*, 5037-5046, 1986.

Levitus, S., *Climatological Atlas of the World Ocean. NOAA Prof. Pap. 13*, 177 pp., National Oceanic and Atmospheric Administration, Boulder, Colo., 1982.

Maier-Reimer, E., and R. Bacastow, Modelling of geochemical tracers in the ocean, in *Climate-Ocean Interaction*, edited by M. E. Schlesinger, pp. 233-267, Kluwer, Dordrecht, 1990.

Maier-Reimer, E., and K. Hasselmann, Transport and storage of CO_2 in the ocean – An inorganic ocean-circulation carbon cycle model, *Climate Dyn., 2*, 63-90, 1987.

Maier-Reimer, E., and U. Mikolajewicz, Experiments with an OCGM on the cause of the Younger Dryas, *Max Planck Institut für Meteorologie, Hamburg, Germany, 39*, 13 pp., 1989.

Manabe, S., and R. J. Stouffer, Two stable equilibria of a coupled ocean-atmosphere model, *J. Climate, 1*, 841-866, 1988.

Marotzke, J., and J. Willebrand, Multiple equilibria of the global thermohaline circulation, *J. Phys. Oceanogr., 21*, 1372-1385, 1991.

Marotzke, J., P. Welander, and J. Willebrand, Instability and multiple equilibria in a meridional-plane model of the thermohaline circulation, *Tellus Ser. A, 40*, 162-172, 1988.

Stocker, T. F., and D. G. Wright, Rapid transitions of the ocean's deep circulation induced by changes in surface water fluxes, *Nature, 351*, 729-732, 1991a.

Stocker, T. F., and D. G. Wright, A zonally averaged ocean model for the thermohaline circulation, Part II, Interocean circulation in the Pacific-Atlantic basin system, *J. Phys. Oceanogr., 21*, 1725-1739, 1991b.

Stocker, T. F., D. G. Wright, and L.A. Mysak, A zonally averaged, coupled ocean-atmosphere model for paleoclimatic studies, *J. Climate, 5*, 773-797, 1992.

Stommel, H., and A. B. Arons, On the abyssal circulation of the world ocean, II, An idealized model of the circulation pattern and amplitude in oceanic basins, *Deep Sea Res., 6*, 217-233, 1960.

Toggweiler, J. R., K. Dixon, and K. Bryan, Simulations of radiocarbon in a coarse-resolution world ocean model, 1, Steady state prebomb distributions, *J. Geophys. Res., 94*, 8217-8242, 1989.

Weyl, P. K., The role of the oceans in climatic change: A theory of the ice ages, *Meteorol. Monogr., 8*, 37-62, 1968.

Wright, D. G., and T. F. Stocker, A zonally averaged ocean model for the thermohaline circulation, Part I, Model development and flow dynamics, *J. Phys. Oceanogr., 21*, 1713-1724, 1991.

Wright, D. G., and T. F. Stocker, Sensitivities of a zonally averaged global ocean circulation model, *J. Geophys. Res.*, in press, 1992.

W. S. Broecker and T. F. Stocker, Lamont-Doherty Geological Observatory, Palisades, NY 10964.

D. G. Wright, Bedford Institute of Oceanography, Department of Fisheries and Oceans, Dartmouth, Nova Scotia, Canada.

(Received April 14, 1992;
revised June 26, 1992;
accepted July 14, 1992.)